The Topological Casimir Effect on a Torus

by

Moos van Caspel

A THESIS SUBMITTED IN PARTIAL FULFILLMENT OF
THE REQUIREMENTS FOR THE DEGREE OF

MASTER OF SCIENCE

in

THE FACULTY OF GRADUATE AND POSTDOCTORAL STUDIES

(Physics)

THE UNIVERSITY OF BRITISH COLUMBIA

(Vancouver)

August 2013

Abstract

The conventional Casimir effect manifests itself as a quantum mechanical force between two plates, that arises from the quantization of the electromagnetic field in the enclosed vacuum. In this thesis the existence is discussed of an extra, topological term in the Casimir energy at finite temperatures. This topological Casimir effect emerges due to the nontrivial topological features of the gauge theory: the extra energy is the result of tunneling transitions between states that are physically the same but topologically distinct. It becomes apparent when examining, for instance, periodic boundary conditions. I explicitly calculate the new term for the simplest example of such a system, a Euclidean 4-torus. By dimensional reduction, this system is closely related to two dimensional electromagnetism on a torus, which is well understood. It turns out that the topological term is extremely small compared to the conventional Casimir energy, but that the effect is very sensitive to an external magnetic field. The external field plays the role of a topological theta parameter, analogous to the θ vacuum in Yang-Mills theory. The topological Casimir pressure and the induced magnetic field show a distinctive oscillation as a function of the external field strength, something that can hopefully be observed experimentally.

Preface

Most of the content in this thesis has been previously published in a paper [1], co-written by my collaborator ChunJun (Charles) Cao, my supervisor Ariel Zhitnitsky and myself. This being theoretical physics, I think it is fair to say that the three of us were involved in all parts of the research, through discussions and thorough editing cycles of the paper. Parts that I did not contribute to, like the appendix, have not been reproduced here but are only cited. Bits and pieces from the rest of the publication have found their way into this work, but the vast majority has been rewritten in order to cater to a wider audience. I believe that this thesis will be readable to any graduate student with a basic knowledge of quantum field theory, not just to experts in the field. Hopefully this will make it easier for a new student to continue our research in the future, helping them answer the questions that we have asked ourselves over the last year. Aside from the computations that can be found in the published paper, I have added a significant amount of material to put the research in a broader perspective of physics — including a discourse on related topological systems and two appendices.

Charles Cao created the numerical plots in section 5, which have been reproduced here with his explicit permission. I want to thank him for our many discussions, and for his pleasant company on the travels to present our work at several conferences. It was a joy working with him. I am also very grateful to professor Ariel Zhitnitsky, for proposing and supporting this research during the two years of my MSc program. It was inspiring to work on something so new and exciting, and to get rewarded for our effort with a publication.

Moos van Caspel, 2013

Contents

List of Figures

1 Introduction

The idea of a mysterious quantum force, arising purely from the vacuum, was a controversial issue for several decades. When Hendrik Casimir first predicted his eponymous effect [2] in 1948, the existence of vacuum fluctuations was not yet well established. Quantum field theory was still in its early development. Later theoretical advances brought a better understanding of the quantum vacuum and the Casimir effect became a well-studied part of physics. Regardless, it took nearly 50 years before the effect was quantitatively measured in an experiment [3], although qualitative confirmation of the Casimir force was achieved in the '70s.

The Casimir effect arises from the quantization of fields under boundary conditions. Within the boundary only certain field modes are allowed, providing a vacuum energy that is different than in free Minkowski space. This energy difference is dependent on the size of the system, such that a real force is generated on the boundary. The famous example, as first studied by Casimir, is that of two parallel, perfectly conducting plates. Even in a perfect vacuum, these neutral plates feel an attractive force that is purely of quantum mechanical origin. The Casimir energy for this system is given by

$$E_{\mathrm{C}} \;\equiv\; (E_{\mathrm{BC}} - E_{\mathrm{Minkowski}}) \;=\; -\,\frac{\hbar\, c\, \pi^2\, L^2}{720\, a^3}, \tag{1}$$

where a is the separation distance between the plates of length L. Since the system can lower its energy by decreasing a, this results in the well-known Casimir pressure

$$P \;=\; -\,\frac{1}{L^2}\cdot\frac{\partial E_{\mathrm{C}}}{\partial a} \;=\; -\,\frac{\hbar\, c\, \pi^2}{240\, a^4}. \tag{2}$$

The pressure rapidly falls off with distance and becomes typically relevant on micrometer scales or smaller. That is why there has been an increased interest in the Casimir effect with the recent advent of nanotechnology.

Since its original prediction, the Casimir effect has been studied for many different configurations and many different fields [4]. In addition to physical boundaries like metal plates, the effect can also occur on nontrivial topological spaces. For example, the periodicity of space can produce a similar field quantization as the conducting plates and will also produce a vacuum pressure. Typically these calculations are done for simple scalar fields. While the electromagnetic field is more relevant for experiments, it can often be

reduced to a scalar field computation by treating the two polarization directions separately.

There are however situations in which the electromagnetic field can produce a unique kind of vacuum effect, that cannot be described in terms of scalar fields. One of these is the *topological Casimir effect* , in which an additional vacuum pressure arises due to the gauge invariance of the field, when defined on a topologically nontrivial manifold. Whereas the conventional Casimir effect results from the vacuum fluctuations of physical photons, the topological effect is solely due to a new type of excitations, known as instantons.[1]

In the topological Casimir effect, mappings between the gauge group and the spacetime topology create an infinite number of degenerate vacuum states. These so-called topological sectors correspond to the same physical state, even though they are topologically distinct. The instanton excitations, which contribute to the system's vacuum energy, can be interpreted as tunneling events between the vacuum states. Because the topological Casimir effect has an entirely different source than the conventional photon fluctuations, it shows some fascinating behavior that is worth studying. Examples include a sensitivity to external magnetic fields and possible applications in cosmology.

It should be noted that this is not the first time that the vacuum energy is computed for the electromagnetic field on nontrivial topological spaces. Earlier this year, Gerard Kelnhofer formulated the theory for a general compact manifold, in a very formal mathematical manner [6]. However, he does not discuss any of the physical consequences of the topology. Older papers suggest that it is necessary to sum over topological sectors, but did not perform the calculations [7]. In this work, I will focus on an intuitive understanding of the problem, discussing the physical context and the possibility of experimental observation. Recreating the topological Casimir effect in a lab would be a unique opportunity to probe the topological properties of the quantum vacuum in a controlled environment, but there are many challenges involved that need to be considered.

This thesis follows largely the structure of our recent paper [1], with

[1] A remark must be made here on the terminology. In some older literature, the regular Casimir effect on a topological space is also called the 'topological Casimir effect'. However, in this work the term is used in a much stricter sense. Here the topological Casimir effect arises purely from topological fluctuations, instead of real propagating degrees of freedom like photons. For the latter, I will use the term *conventional Casimir effect*, to distinguish it from the newly discussed topological contributions. This naming convention was first used in [5].

the addition of some extra background material. This material serves to put the topological Casimir effect in a broader light and to show some of the motivation for this work. As a matter of fact, the topological Casimir effect is very closely related to other systems in physics, sharing the same underlying mathematics. In section 2, I will start with a brief explanation of some of this math and discuss two important examples of topology in physics: the Aharonov-Bohm effect and the Yang-Mills vacuum. Both are directly analogous to the systems that are examined later in the text, and I will regularly refer back to these examples.

In section 3 I review a toy model for the topological Casimir effect, namely 2d electrodynamics on a circle — a well-studied system with a lot of literature. In two spacetime dimensions, photons cannot exist. This means that there is no conventional Casimir effect, which would be caused by the zero-point energy of the photon modes. Nevertheless, we will see that there are topological excitations that give the theory its vacuum energy. These 2d instantons can be easily generalized to higher dimensions in order to describe the 4d topological Casimir effect.

By generalizing the 2d electromagnetic theory, the topological Casimir effect is formulated on a Euclidean 4-torus in section 4. In this case, it can be shown that the topological and conventional part of the vacuum energy are completely separated. Since the conventional Casimir effect can be computed through known methods, I will focus on the topological part. This part can be related to the 2d theory from section 3 by using the technique of dimensional reduction, allowing us to directly apply the previous results to this new system. Unfortunately, the topological pressure turns out to be very small, compared the conventional Casimir force. Without some kind of characteristic behavior, it is unlikely that the topological Casimir effect can be measured.

We are in luck, because the topological Casimir effect interacts with an external magnetic field in a very specific manner, as discussed in section 5. While the conventional Casimir effect is unchanged by the application of an external field, the topological pressure shows an interesting oscillatory behavior as a function of the field strength B_{ext}. In fact, the external magnetic field plays the role of a topological theta parameter, in close analogy with the examples from section 2. Under the influence of this theta parameter, the energy of the instanton configurations is shifted and they will create an induced magnetic field. The induced field and the corresponding magnetic susceptibility also show an unusual variation as B_{ext} is changed. Hopefully this can be use to the distinguish the topological Casimir effect from the conventional one.

Section 6 concludes this work with a short discussion on experimental considerations and future directions for the topological Casimir effect. While this is a theoretical paper, I think it is important to keep in mind our reliance on observational data to confirm these new concepts. I cannot complete this thesis without exploring some of these practical aspects of the effect. Finally in the Appendix, I review the conventional Casimir effect and discuss a few mathematical tools that are used throughout the text.

2 Topological Sectors and Winding Numbers

Topology has been a booming subject within physics in the last decade. It is an abstract field of mathematics, and as such its applications are often not obvious. But in recent years it has become clear that in a wide range of physics, from condensed matter to high energy, the consequences of topology cannot be ignored; it can, in fact, lead to some very interesting phenomena. The greatest example is the rapid development in the theory of topological insulators, which started in 2005 and still sees many new publications each week.

Although topological effects can be found in many areas of physics, they all have certain features in common. This universality is a result of the underlying mathematical principles, which I will discuss briefly in this section. This will be, when possible, from a physicist's point of view, choosing intuitive understanding over mathematical rigor. For a more mathematical approach, see [8].

2.1 Homotopy 101

Two spaces are topologically equivalent (or homotopic) if you can continuously deform one into the other, without cutting them or gluing parts together. The canonical example is the donut and the coffee mug, which have the same topology: the donut's hole turns into the handle of the mug. However, the donut is inequivalent to a ball, since one cannot remove the hole in a continuous deformation.

It is clear that the number of holes in a space is important for the topology. This is however not a very well-defined quantity, especially in higher dimensions. Therefore we introduce *homotopy groups*. These groups, labeled by π_n, consist of the mappings between the topological space and the n-sphere S_n. The first homotopy group, also known as the fundamental group π_1, has a fairly intuitive definition in terms of loops: its elements are unique loops that cannot be continuous deformed into one another.

For example, a space with one hole through it (like the circle S^1) can contain loops that wrap around this hole an integer number of times, see figure 1. Loops with different winding numbers are topologically distinct and correspond to different elements of the fundamental group. As a result, we can conclude that $\pi_1(S^1) \simeq \mathbb{Z}$. A torus $\mathbb{T}^2 \equiv S^1 \times S^1$ has two independent winding numbers, one for each circle, yielding $\pi_1(\mathbb{T}^2) \simeq \mathbb{Z}^2$. Contrarily, on a sphere S^2 any loop can be contracted to a point, such that $\pi_1(S^2) \simeq 0$. If all homotopy groups of a space are empty, as is the case with Euclidean or

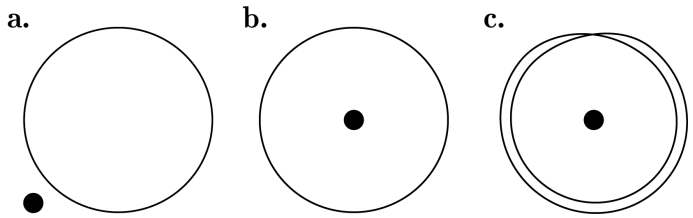

Figure 1: *Illustration of loops with different winding numbers. The black dot represents a hole in the space, such that a loop cannot pass it when being continuously deformed.* **a**: $n = 0$. *The loop can be continuously contracted to a single point.* **b**: $n = 1$. *The loop wraps once around the hole, it cannot be contracted to a point.* **c**: $n = 2$. *The loop wraps twice around the hole.*

Minkowski space, the space can be considered topologically trivial.

In general it can be very hard to compute the homotopy groups of a given space, but in the context of physics this is typically not necessary. We will see that the previous example, where the fundamental group is equivalent to the integers, is in fact of the most interest to us. The integers correspond to the so-called topological sectors, which play an important part in the topological Casimir effect. In the rest of this section I will discuss two famous instances of topological sectors in physics that will demonstrate two related concepts: theta states and instantons.

2.2 The Aharonov-Bohm Effect: Theta States

While often covered in basic quantum mechanics classes, it might be a surprise to some that the Aharonov-Bohm effect is topological in nature. An electron moving around a solenoidal magnet will acquire a complex phase, even though it does not pass through any electromagnetic field. To show the role of topology, let us confine the electron to a circle around this magnet, so that its movement can be described by the angular coordinate ϕ. The classical action is given by

$$S[\phi] = \int \mathrm{d}t \left(\frac{m_e}{2} \dot{\phi}^2 + \frac{\theta}{2\pi} \dot{\phi} \right), \qquad \theta \equiv \frac{e}{\hbar c} \Phi \tag{3}$$

with Φ the flux through the solenoid. It is immediately clear that the second term is a full derivate and thus depends only the beginning and end position of the electron. This is characteristic of a topological term in the action: it does not depend on the path taken. With every full circle clockwise, the term increases by θ.

In classical mechanics, the topological term would not contribute to the equations of motion. However, after canonical quantization we find the energy eigenvalues to be

$$E_n = \frac{1}{2m_e}\left(n - \frac{\theta}{2\pi}\right)^2, \qquad n \in \mathbb{Z}, \tag{4}$$

where we work in natural units $\hbar = c = 1$ from here on. The spectrum is shifted, depending on θ, but note that there is a 2π periodicity. The corresponding eigenfunctions are $\psi_n = e^{in\phi}$, showing the familiar phase change as the electron moves around.

The problem becomes more interesting when we add a finite temperature and view it as a quantum statistical system. In this case we need to compute the partition function, defined by the path integral

$$Z = \int \mathcal{D}\phi \; e^{iS[\phi]} = \int_E \mathcal{D}\phi \; e^{-S_E[\phi]}. \tag{5}$$

In the second expression we have switched to Euclidean space by means of a Wick rotation (see appendix B.1). The rotated time $\tau \equiv -it$ is periodic with period β, which means that all paths must satisfy $\phi(\beta) - \phi(0) = 2\pi k$, for some integer k. This integer is known as the *winding number*, as it counts the number of loops around the circle during one time period. In the partition function one must sum over all winding numbers.

With this, the Euclidean action becomes:

$$S_E = \int_0^\beta \mathrm{d}\tau \left(\frac{m_e}{2}\dot{\phi}^2 - i\frac{\theta}{2\pi}\dot{\phi}\right) = -i\theta k + \int_0^\beta \mathrm{d}\tau \frac{m_e}{2}\dot{\phi}^2 \tag{6}$$

where we have made use of the topological term as a total derivative. Inserting this into the path integral, we can write

$$Z = \sum_k e^{i\theta k} \int_{\phi(\beta)-\phi(0)=2\pi k} \mathcal{D}\phi \; e^{-\frac{1}{2}\int_0^\beta \mathrm{d}\tau \; m_e\dot{\phi}^2}. \tag{7}$$

This final form shows very clearly the physics of the system: the partition function is a sum over path integrals in different *topological sectors*, which are represented by the winding number k. The winding numbers originate from the mapping of the paths onto the circle, or $\pi_1(S^1) \simeq \mathbb{Z}$.

The topological θ-term emerges as a complex weight of the topological sectors. Although θ has a specific physical meaning in this case, i.e. the magnetic flux through the system, its role in topological effects is very universal; we shall see several other examples. An important remark is that even at $\theta = 0$, the topological sectors still contribute to the partition function.

2.3 The Yang-Mills Vacuum: Instantons

Yang-Mills theory is a non-Abelian gauge theory that forms the basis for the description of the weak and strong forces in the Standard Model. Here we will work with the SU(2) gauge group, since it is generated by the familiar Pauli spin matrices. In the vacuum state, the potential must be a pure gauge configuration as given by:

$$A_\mu = \frac{i}{g} U(\mathbf{x})\, \partial_\mu U^\dagger(\mathbf{x}) \ , \qquad U(\mathbf{x}) \in \mathrm{SU}(2) \tag{8}$$

where g is the coupling constant and we have fixed our gauge such that $A_0 = 0$. This defines the gauge U on $\mathbb{R}^3$. However, by assuming that U is constant at infinity, the boundary is shrunk to a point and the space is compactified into a 3-sphere S_3. That leaves us with the mapping $U : S^3 \to \mathrm{SU}(2)$, which can conveniently be characterized by the homotopy group $\pi_3(\mathrm{SU}(2)) \simeq \mathbb{Z}$.

Physically, that means that every gauge U can be assigned an integer winding number, that signifies how many times $U(\mathbf{x})$ wraps around the spatial 3-sphere. Gauges with different winding numbers cannot be continuously deformed into each other. The consequences of this are very deep: configurations of pure gauges with different winding numbers must be separate, local minima of the Hamiltonian. After all, when deforming one into the other we must pass through configurations that do not correspond to a pure gauge, and thus have a nonzero energy. See [9] for details.

These local minima provide an infinite number of topologically distinct vacuum states $|n\rangle$, known as the topological sectors of the theory. They are connected by gauge transformations with a nonzero winding number, also known as *large gauge transformations* (LGTs). The result is sometimes called a degeneracy of the vacuum, but one must take care not to confuse it with the regular definition of degeneracy in quantum mechanics - these local minima all correspond to the same physical state, despite being topologically different. In fact, the generic ground state of the system can be written as

$$|\theta\rangle = \sum_n e^{-i\theta n} |n\rangle. \tag{9}$$

This is known as the theta vacuum, and the similarities to eq. (7) are striking: again θ serves as the complex weight of the topological sectors. Indeed, the θ parameter would appear in the Yang-Mills Lagrangian density as the topological term

$$\mathcal{L}_{top} = \frac{ig^2\theta}{16\pi^2}\, \tilde{F}^{\mu\nu} F_{\mu\nu} \tag{10}$$

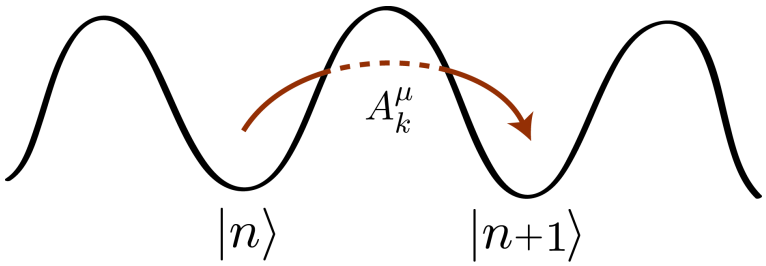

Figure 2: *As a result of mappings between the gauge group and the space-time topology, there are an infinite number of winding states $|n\rangle$ corresponding to local minima of the Hamiltonian. These degenerate vacuum states are topologically different, even though they resemble the same physical state. An instanton configuration A_k^μ of topological charge k represents tunneling between these topological sectors.*

with $\tilde{F}^{\mu\nu} = \frac{1}{2}\epsilon^{\mu\nu\sigma\tau}F_{\mu\nu}$ being the dual field strength. Just as in the Ahoronov-Bohm effect, this term is a total derivative, such that the action depends only on the boundary conditions. It does not contain the metric tensor, another characteristic property of topological terms. In quantum chromodynamics, the apparent lack of such a term is known as the *strong CP problem*.[2]

If all the winding states $|n\rangle$ correspond to the same physical state, then what are the consequences of this topological vacuum structure? The most important feature is a new type of excitations, called *instantons*. Instantons represent tunneling through the energy barriers between vacuum states - they are non-perturbative, classical solutions to the Euclidean equations of motion. When solving a double-well problem in the path integral approach, instantons will emerge. In the case of the Yang-Mills vacuum, there can be tunneling between any two vacua $|n\rangle$ and $|n'\rangle$, giving the corresponding instanton a so-called topological charge $k = n - n'$. See figure 2.

Instantons play a crucial role in the rest of this thesis. They are real, topological excitations that need to be taken into account when computing partition sums and expectation values. In the next section we will show that instantons can arise in electrodynamics, we will explicitly construct them and see how they will lead to the topological Casimir effect.

[2] A nonzero theta term in the QCD Lagrangian would be a large source of $\mathcal{CP}$-violation in the strong sector. That makes it possible to measure θ with great precision and the current experimental upper limit is $|\theta| < 2 \times 10^{-10}$. Because there are no symmetry arguments why the term should vanish, this poses a fine-tuning problem.

3 Electromagnetism in Two Dimensions

Before arriving at the topological Casimir effect, it is instructive to study a much simpler system: Maxwell electrodynamics on a two-dimensional, compact spacetime. This is a well-understood problem, but it will prove to be an exceptionally good toy model for topological effects in higher dimensions. Even better, we will be able to generalize our computations from this section to four-dimensional spacetime and use them to describe the TCE.

With two spacetime dimensions, the theory of electromagnetism is quite different than what we are used to. The most interesting property is that electromagnetic waves cannot exist in just one spatial dimension. After all, the Maxwell equations require that the polarization of an EM-wave be perpendicular to its direction of propagation. As a result, the wave equation has no solution other than the zero mode. In terms of quantum field theory, this means that the model has no photons and is completely devoid of physical propagating degrees of freedom. In that sense the theory can be considered "empty". However, we will see that when formulating the theory on a circle, topological excitations will emerge — much like the instantons in section 2.3.

In the Yang-Mills vacuum, the existence of topological sectors and instantons is due to the mapping between the compactified Euclidean space and the gauge group, characterized by $\pi_3(\mathrm{SU}(2)) \simeq \mathbb{Z}$. On the other hand, in the 2d Maxwell theory we have a mapping between the one dimensional compactified space S_1 and the Abelian gauge group U(1). Here too we find a nontrivial vacuum structure, given by $\pi_1(\mathrm{U}(1)) \simeq \mathbb{Z}$. The tunneling between these topological sectors is what provides the theory with its energy spectrum and its interesting features.

A more intuitive way to view the topological sectors is to consider periodic boundary conditions, up to a gauge.

$$A_\mu(L,t) = A_\mu(0,t) + \partial_\mu \alpha \tag{11}$$

where L is the size of the space and α is some scalar function. However, an electron field would pick up a phase $e^{ie\alpha(x)} \in \mathrm{U}(1)$ under this gauge transformation. If we require the matter field to be single valued on the circle, this puts certain restrictions on the allowed gauges, for example

$$\alpha = \frac{2\pi k}{eL}\, x\,, \qquad k \in \mathbb{Z}. \tag{12}$$

In other words, the periodicity of the matter field quantizes the allowed gauges α. For $k \neq 0$, α represents a large gauge transformation of winding

number k, as mentioned in section 2.3. We shall see below that the boundary condition (11) is satisfied by a classical instanton configuration of topological charge k. Again one has to sum over all allowed k in the partition sum, to include all excitations in the system. The topological features of the theory arise very naturally in this way.

Two-dimensional electromagnetism on a circle is also known as the Schwinger Model without fermions, which has been solved in a number of different ways [10]. The presence of instanton configurations in this model is well established and in fact has been shown to be required for a consistent theory [1]. Without the contribution of the topological sectors, the Schwinger model would violate the Ward Identities, one of the most fundamental statements about symmetries in quantum field theory.

Because the model is so simple, it is possible to do the canonical quantization and compute all quantities using the Hamiltonian approach. It is however more useful for us to take the path integral approach, which is much easier to generalize to higher dimensions. We will discuss both methods below.

3.1 Hamiltonian Approach

The Hamiltonian approach is exactly like the analysis in section 2.2 of the electron on a circle. The single zero mode of the electromagnetic field plays the role of the particle. To see this, we fix the gauge as follows

$$A_0 = 0, \qquad \partial_1 A_1 = 0. \tag{13}$$

This means the scalar electric field is given by $E = \dot{A}_1$. There can be no magnetic field in one spatial dimension, since the vector cross product has no meaning. Classically, Gauss' Law implies that $\partial_x E = 0$, which shows that we are dealing only with one x-independent zero mode. As mentioned earlier, no physical propagation degrees of freedom can exist in this system, as there can be no polarization perpendicular to the momentum.

We can then quantize the theory, taking A_1 and E as canonical conjugates:

$$[A_1(x), E(x)] = i\hbar\,\delta(x-y). \tag{14}$$

The periodic boundary conditions are due to the identification of the gauge equivalent configurations

$$A_1 \approx A_1 + \frac{2\pi n}{eL}\,, \qquad n \in \mathbb{Z} \tag{15}$$

as discussed above. With that, the rescaled variable eA_1L takes the place of the coordinate ϕ in the Aharonov-Bohm effect of section 2.2. By perfect analogy, the conjugate momentum is quantized $E = en$ and the Hamiltonian with its energy eigenvalues becomes

$$H = -\frac{1}{2L} \cdot \frac{d^2}{dA_1^2}\,, \quad E_n = \frac{1}{2} n^2 e^2 L. \tag{16}$$

In studies of the Schwinger model it is also customary to add a theta parameter, although the interpretation is not as clear as in the Aharonov-Bohm effect, where it represents magnetic flux. The parameter enters the computations in the same way, by shifting the energy levels:

$$E_n = \frac{1}{2} e^2 L \left(n + \frac{\theta}{2\pi} \right)^2 . \tag{17}$$

Including the theta term, the thermal partition sum takes the following form

$$\mathcal{Z}(\theta) = \sum_{n \in \mathbb{Z}} e^{-\beta E_n} = \sum_{n \in \mathbb{Z}} e^{-\frac{1}{2} e^2 L \beta \left(n + \frac{\theta}{2\pi} \right)^2}, \tag{18}$$

where β is the inverse temperature. We will now derive this same result using Euclidean path integral calculations, in which the role of the instantons is much more obvious.

3.2 Path Integral Approach

By performing a Wick rotation, we can define the same theory on the Euclidean torus of size $L \times \beta$. See appendix B.1. In this formulation the appearance of topological sectors becomes immediately clear. In order to satisfy the boundary conditions (11, 12), we can introduce the classical instanton-like potential

$$A_0^{(k)} = 0\,, \qquad A_1^{(k)} = \frac{2\pi k}{eV}\, x_0, \tag{19}$$

where $V = L\beta$ is the volume of the Euclidean space. The integers k classify the instantons, which represent transitions between the topological sectors. The field strength of the classical configuration is given by

$$E^{(k)} = \partial_0 A_1^{(k)} = \frac{2\pi k}{eV}. \tag{20}$$

Please note that this E-field should not be confused with the real electric field that was derived in Minkowski space with the Hamiltonian approach.

Instead, (20) is an unphysical, complex configuration in Euclidean space with no clear interpretation. It is proportional to the so-called topological charge density $Q = \frac{e}{2\pi} E^{(k)}$ such that the integral

$$\int \mathrm{d}^2x \; Q(x) = \frac{e}{2\pi} \int \mathrm{d}^2x \; E^{(k)}(x) = k \tag{21}$$

is the topological charge of the instanton.

For the path integral, we split the potential into the classical configuration plus the quantum fluctuations around it: $A_\mu = A_\mu^{(k)} + \delta A_\mu$. The fluctuating field δA_μ must satisfy periodic boundary conditions, such that the action $S = \frac{1}{2} \int \mathrm{d}^2x \, E^2$ can also be split into a classical and a quantum part - the cross terms vanish when integrating the full derivative. As a result, the partition function can be written as

$$\mathcal{Z} = \sum_{k\in\mathbb{Z}} \int \mathcal{D}A \; e^{-\frac{1}{2}\int \mathrm{d}^2x \, E^2} = \; \mathcal{Z}_q \sum_{k\in\mathbb{Z}} e^{-\frac{2\pi^2 k^2}{e^2 V}}, \tag{22}$$

where the exponentials represent the classical instanton configurations and the prefactor

$$\mathcal{Z}_q = \int \mathcal{D}\delta A_1 \; e^{-\frac{L}{2}\int \mathrm{d}^2x \; \delta\dot{A}_1^2} \tag{23}$$

is the path integral over the fluctuating field. By the same reasoning as in the Hamiltonian approach, the $A_0 = 0$ gauge implies that δA_μ is x-independent., which makes the computation of $\mathcal{Z}_q$ a simple quantum mechanical problem.

$$\mathcal{Z}_q = \int \mathcal{D}\delta A_1 \; e^{-\frac{L}{2}\int_0^\beta d\tau (\delta\dot{A}_1)^2} = \int \mathcal{D}\delta a_1 \; e^{-\frac{L}{2}\left(\frac{2\pi}{eL}\right)^2 \int_0^\beta d\tau (\delta\dot{a}_1)^2} \tag{24}$$

where in the second step we have changed integration to the dimensionless variable $\delta a_1 = \frac{eL}{2\pi} \delta A_1$, which fluctuates between 1 and 0 according to (15). This makes the partition sum equivalent to that of a free particle with mass $m \equiv L\left(\frac{2\pi}{eL}\right)^2$ and for this Gaussian path integral the result is known to be

$$\mathcal{Z}_q = \sqrt{\frac{m}{2\pi\beta}} = \sqrt{\frac{2\pi}{e^2 V}}. \tag{25}$$

Inserted into eq. (22), this gives the full partition sum.

In Euclidean space, the topological θ-term enters the partition function as the complex weight of the topological sectors, just like we saw in section 2.2. The final result is

$$\mathcal{Z}(\theta) = \; \sqrt{\frac{2\pi}{e^2 V}} \sum_{k\in\mathbb{Z}} e^{-\frac{2\pi^2 k^2}{e^2 V} + ik\theta}. \tag{26}$$

This expression is exactly the same as the result obtained by the Hamiltion approach in (18), as can be seen by applying the Poisson resummation formula (see appendix B.2). The two forms are said to be dual. See [11] for a more detailed comparison between the Hamiltonian and the path integral approach of the Schwinger model.

One thing of note about the partition sum (26) is that it converges. Unlike the conventional Casimir effect, here there is no need for a regularization scheme. While there is no closed form for the expressions (18, 26), they correspond to a special function that is well studied: the Jacobi Theta function Θ. The two dual forms are very usual for studying the asymptotic behaviour of the system, for example in the low temperature limit.

3.3 Interpretation

From the partition function it is easy to calculate the free vacuum energy $F = -\frac{1}{\beta} \ln \mathcal{Z}$ and any other thermodynamic quantity. Expressions (18, 26) show clearly that the free energy depends on the size of the system L, just like in the conventional Casimir effect. This is crucial for our work, since it holds the promise of a measurable effect: the vacuum pressure on the system. The system could lower its energy by moving the boundaries, providing a real force.

In the conventional Casimir effect, the vacuum pressure arises from the zero-point energy of the electromagnetic field modes, i.e. the photons. However, in our two-dimensional system these photonic modes do not exist and as such cannot contribute to the zero-point energy. What then causes this pressure that our computations suggest? This energy comes from topological excitations at a nonzero temperature, rather than the regular propagating degrees of freedom. These excitations, or instanton configurations (19), can be interpreted as the tunneling transitions between degenerate vacuum states. The vacuum states all correspond to the same physical state, but are topologically distinct and related to each other by large gauge transformations like (12).

The energy associated with the tunneling processes is dependent on the topological charge (21), or the separation between the topological sectors. It is also the energy of this tunneling that depends on the system's size, providing the theory with what we call *the topological Casimir effect* - a vacuum pressure purely caused by topological degrees of freedom. The underlying cause of this effect is the interaction between the gauge field and a nontrivial compact spacetime manifold, characterized by the fundamental group $\pi_1(\mathrm{U}(1)) \simeq \mathbb{Z}$. This means that it can never be reduced to a problem

in terms of scalar fields, a technique that is often used in the conventional Casimir effect (see appendix 6).

The question is whether this effect would be really measurable, or whether it is just a mathematical glitch that can be removed by renormalization or the redefinition of variables. After all, if the degenerate vacua correspond to the same physical state, then why should tunneling between them result in a physical effect? This is a question that has plagued physicist ever since the Yang-Mills vacuum was first studied. However, as mentioned before there is clear evidence from the Schwinger model that topological sectors are real and must be taken into account for a consistent theory [1].

Another concern is whether the topological effects in this section are just an interesting quirk of two-dimensional spacetime. Since we live in four spacetime dimensions, this would mean that the effect is irrelevant for any experimental measurement, no matter how interesting the theory is. Fortunately, the topological Casimir effect is much more general than that and the next section deals with its description in 4d. Many of the computations from this section will carry over, yielding a very simple model that may allow the measurement of topological vacuum effects in the lab.

4 Topological Casimir Effect in Four Dimensions

In two-dimensional electromagnetism, the nontrivial structure of the vacuum arises due to the mapping of the gauge group U(1) onto the manifold S^1. A naive generalization to 4d spacetime would follow the reasoning of section 2.3, by compactifying the Euclidean space to S^3. Unfortunately this does not work: while S^3 is not topologically trivial, its mappings to U(1) are. In the language of homotopy groups, we can write $\pi_3(\mathrm{U}(1)) \simeq 0$, meaning that on this manifold all the gauges can be continuously transformed into one another. There will be no degenerate vacua, no tunneling and no topological Casimir effect. In order to recover the topological vacuum effects in higher dimensions, we need to look at different manifolds — like those with a toroidal topology.

Consider a four-dimensional Euclidean box, of size $\beta \times L_1 \times L_2 \times L_3$. When we apply periodic boundary conditions to the opposing sides of the box, this creates a space with the topology of a 4-torus $S^1 \times S^1 \times S^1 \times S^1$. This manifold does provide topologically nontrivial mappings to the gauge group U(1), and in fact there are several independent winding numbers that count the wrapping around the different loops on the torus. The calculations for this system are difficult and have been done in [6]. However, we can make some assumptions that will greatly simplify the theory, allowing us to describe the 4d topological effects in terms of the 2d computations.

If we assume that L_3 is much smaller than L_1 and L_2, this suppresses the contribution of all but one of the winding numbers, for reasons that will become clear below. Taking a slice of this system in the xy-plane now precisely recovers the topological features of the 2d Schwinger model, a technique known as *dimensional reduction*. It also simplifies the calculation of the propagating degrees of freedom, analogous to the simple example of two large parallel plates in the conventional Casimir effect. In fact it is rather tempting to interpret this 4-torus simply as two large parallel plates with periodic boundary conditions, at finite temperature.

These two portions of the vacuum energy, resulting from the topological sectors and the physical photons respectively, are completely decoupled in this system. This means that the two contributions can be computed separately. Convenient, since the conventional Casimir effect for these boundary conditions has been studied many times. I have nothing new to add there and the details are discussed in appendix A.2. Most of this section will consequently focus on the topological part, such that in the end we can compare its effects to the conventional vacuum pressure.

4.1 Decoupling of the Topological and Conventional Parts

It is not difficult to generalize the 2d instanton potential (19) to higher dimensions. The boundary conditions (11, 12) are more or less unchanged, but can be applied in any of the directions. One way we can define the classical instanton configurations is

$$A^{\mu}_{top} = \left(0,\ -\frac{\pi k}{eL_1L_2}y,\ \frac{\pi k}{eL_1L_2}x,\ 0\right), \tag{27}$$

where k is is the integer-valued topological charge, and L_1, L_2 are the dimensions of the plates in the x and y-directions respectively, which are assumed to be much larger than the distance between the plates L_3. When going around a loop in the xy-plane, this potentional picks up a large gauge transformation that corresponds to tunneling from one topological sector to another, separated by winding number $\Delta n = k$. The configuration provides a topological magnetic flux in the z-direction:

$$\mathbf{B}_{top} = \vec{\nabla} \times \vec{A}_{top} = \left(0,\ 0,\ \frac{2\pi k}{eL_1L_2}\right), \tag{28}$$

in close analogy with the 2d case in eq. (20). Technically, the periodic boundary conditions would also allow different sets of instantons with their own winding numbers, related to loops in different directions. However, the magnetic flux for these configurations would be proportional to $\frac{2\pi}{eL_1L_3}$ or $\frac{2\pi}{eL_2L_3}$, which correspond to a much larger energy because $L_3 \ll L_1, L_2$. Since we are only considering low temperatures, the instantons of eq. (27) would dominate the partition sum such that we can safely neglect all others.

With this, the Euclidean action of the system becomes

$$\frac{1}{2}\int \mathrm{d}^4x \left\{\vec{E}^2 + (\mathbf{B}_q + \mathbf{B}_{top})^2\right\}, \tag{29}$$

where the integration is over the Euclidean torus $L_1 \times L_2 \times L_3 \times \beta$ and $\vec{E}$ and $\mathbf{B}$ are the photonic quantum fluctuations of the electromagnetic field. These terms were not present in the 2d model, but must here be taken into account due to the presence of real propagating physical photons in four dimensions. We find that the action can be easily split into the sum of a topological and a quantum part, because of the vanishing cross term

$$\int \mathrm{d}^4x\ \mathbf{B}_q \cdot \mathbf{B}_{top} = \frac{2\pi k}{eL_1L_2}\int \mathrm{d}^4x\ B_z = 0 \tag{30}$$

Here the fact is used that $\mathbf{B}_q$ is periodic over the domain of integration. As a result, there is no coupling between the conventional quantum fluctuations and the classical instanton potential (27).

As a result, the partition function of the system can be written as $\mathcal{Z} = \mathcal{Z}_0 \times \mathcal{Z}_{top}$ and both parts can be computed separately. The conventional part $\mathcal{Z}_0$ is nothing but the electromagnetic Casimir on the torus, which can be reduced to a simple scalar field calculation. After all, it does not depend on the topological sector k of the theory, so that we can only consider the trivial sector $k = 0$. The resulting expression requires zeta-function regularization, but is not much more difficult to obtain than that for the canonical example of the parralel conducting plates. The details are worked out in appendix A.2. As usual, the conventional Casimir effect manifests itself as a pressure on the plates in the xy-plane due to the zero-point energy of the photon modes, found to be:

$$P_0 = -\frac{2\pi^2}{15L_3^4} \tag{31}$$

at zero temperature. A finite temperature will add a small correction, as computed in appendix A.3.

With the conventional part accounted for, we can now focus purely on the contribution from the topological sectors. For this we will invoke arguments of dimensional reduction to relate our problem to that of section 3. It is then possible to find the topological pressure and compare it to eq. (31), to see whether the topological features of the vacuum result in a measurable effect.

4.2 Computing the Topological Pressure

The instanton potential (27) assumes periodic boundary conditions up to a large gauge transformation, but only in the x and y directions. In other words, all the relevant topological features of the theory live in the xy-plane, which we can consider as a 2-torus. This makes things extraordinarily easy, because the partition sum of topological excitations on a 2-torus is known from section 3. Some minor adjustments have to be made due to the extra dimensions, but most of the work has been done.

Taking 2d slices in the xy-plane recovers the Schwinger model without fermions. Summing over all these slices is done simply by the integral in the 4d action (29). Comparing the instanton configurations (28) and (20), it is

clear that the classical action of the 4d instantons will be slightly different:

$$S_{top} = \frac{1}{2}\int \mathrm{d}^4x \left(\frac{2\pi k}{eL_1L_2}\right)^2 = \frac{2\pi^2k^2\beta L_3}{e^2L_1L_2} \tag{32}$$

as apposed to the 2d action $S_{2d} = \frac{2\pi^2k^2}{e^2\beta L}$. This difference is partly explained by the obvious substitution $L, \beta \rightarrow L_1, L_2$ that follows from the definition of the 2-torus slices. The rest of the disparity can be interpreted as a rescaling of the coupling constant, i.e. the electric charge

$$e_{2d}^2 = \frac{e_{4d}^2}{\beta L_3}, \quad \frac{e^2}{4\pi} \equiv \alpha. \tag{33}$$

This is a common trick of dimensional reduction, and such a redefinition is in fact necessary in order for the units of the actions to be consistent. In 4d, $e^2 \sim \alpha$ is the dimensionless fine-structure constant, whereas in 1+1 dimensions the QED coupling constant has units of $(length)^{-2}$. With the redefinition (33), the two actions are equal. We now apply the same substitutions to the resulting 2d partition function (18, 26) to acquire the 4d expressions:

$$\mathcal{Z}_{top} \;=\; \sqrt{\frac{2\pi\beta L_3}{e^2L_1L_2}}\sum_{k\in\mathbb{Z}} e^{-\frac{2\pi^2k^2\beta L_3}{e^2L_1L_2}} \;=\; \sum_{n\in\mathbb{Z}} e^{-\frac{e^2n^2L_1L_2}{2\beta L_3}}. \tag{34}$$

Again, the two expressions are dual, related by the Poisson resummation formula. We have chosen to take $\theta = 0$, for now, because there is no physical argument for such a term in the Lagrangian. In section 5 we will further investigate how a theta term might emerge in the topological Casimir effect, under the influence of an external magnetic field.

For the purpose of notation is is convenient to introduce the dimensionless parameter

$$\tau \;\equiv\; \frac{2\beta L_3}{e^2L_1L_2} \tag{35}$$

such that the topological partition sum takes the extremely simple form

$$\mathcal{Z}_{top}(\tau) \;=\; \sqrt{\pi\tau}\sum_{k\in\mathbb{Z}} e^{-\pi^2\tau k^2} \;=\; \sum_{n\in\mathbb{Z}} e^{-\frac{n^2}{\tau}}. \tag{36}$$

While this series again has no closed form, there are still some interesting remarks we can make.

Consider the case where the size of the plates becomes infinite, or $L_1 L_2 \to \infty$. Here the parameter τ approaches zero. Using the second expression of eq. (36), we see that all terms vanish, except for the one with $n = 0$. Accordingly, $\mathcal{Z}_{top} = 1$ and all topological features of the theory disappear. Only the conventional Casimir effect $\mathcal{Z}_0$ remains. Also of interest is the asymptotic limit where $\tau \ll 1$. In this case we can include the first nonzero n in the second sum of (36), to find

$$\mathcal{Z}_{top} \approx 1 + 2\, e^{-1/\tau} \ , \quad \tau \ll 1 \tag{37}$$

The pressure on the plates is defined as the derivative of the free energy $F = \frac{1}{\beta} \ln \mathcal{Z}$ towards the separation distance L_3, divided by the area $L_1 L_2$.

$$P_{top} = \frac{1}{\beta L_1 L_2} \cdot \frac{\partial}{\partial L_3} \ln \mathcal{Z}_{top} \tag{38}$$

In the asymptotic limit, the pressure can be calculated analytically from eq. (37). We use the approximation $\ln(1 + 2e^{-1/\tau}) \approx 2e^{-1/\tau}$ to find:

$$P_{top} \approx \frac{e^2}{\beta^2 L_3^2}\, e^{-1/\tau} \ , \quad \tau \ll 1. \tag{39}$$

As expected, the topological pressure is exponentially suppressed in this limit. Comparing this with the conventional Casimir pressure (31), it is clear that the topological effect cannot be measured in this case. Measuring the conventional pressure in the lab is no easy feat, and this contribution is far smaller.

While $\tau \ll 1$ can be examined analytically, it is more interesting to study a system where $\tau \simeq 1$. Is this a reasonable regime, considering the assumption that $L_3 \ll L_1, L_2$? At this point it is useful to look at some numbers, just to get a sense of the orders of magnitude involved. Let us take $L_1 = L_2 = 1\text{mm}$, $L_3 = 0.01\text{mm}$ and a temperature of 1K. Inserting these numbers into eq. (35) gives us $\tau = 0.5$. Such values are not implausible for an experimental measurement and satisfy all our assumptions necessary for using dimensional reduction as well as the low temperature approximation for the conventional Casimir effect. The result is a value for τ that is well outside the asymptotic limit of eq. (39).

Unfortunately there is no analytical expression for P_{top} in the regime where $\tau \simeq 1$ and we must resort to using numerical calculations in order to study its behavior. The series is slow to converge and saturates around $k \sim 1000$. Figure 3 shows the numerical result in the range $0 \leq \tau \leq 3$. The topological pressure on the vertical axis is measured in units of $\frac{2}{e^2 L_1^2 L_2^2}$.

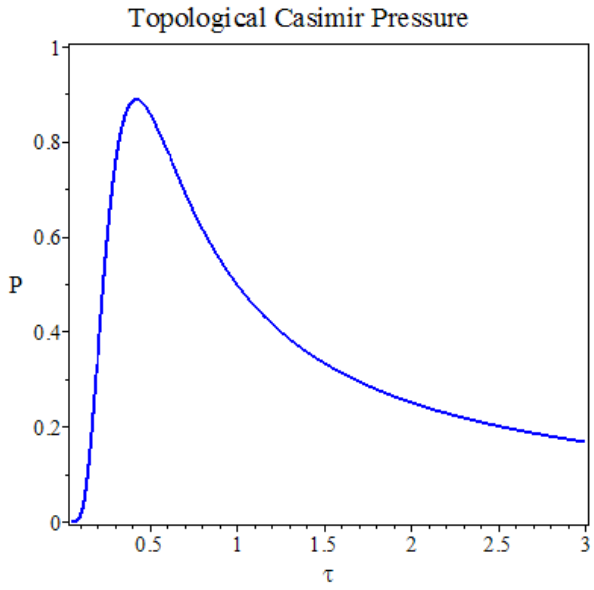

Figure 3: *A numerical plot of the topological pressure in the z-direction on a 4-torus, as a function of* $\tau \equiv 2\beta L_3/e^2 L_1 L_2$. *Pressure is measured in units of* $\frac{2}{L_1^2 L_2^2 e^2}$.

The numerical graph shows several interesting features. First of all, the exponential behavior of eq. (39) when $\tau \to 0$ is clearly reproduced. More important however is the large peak around $\tau \sim 0.4$, where the topology pressure is of order 1 in its given units. It seems that fine-tuning our parameters to reach this maximum is our best bet at producing a measurable effect. The largest topological pressure possible in this system is thus approximately

$$P_{top}^{max} \approx \frac{2}{e^2 L_1^2 L_2^2}. \tag{40}$$

To put this in perspective, let us compare this result with the conventional Casimir effect of eq. (31). It is enlightening to look at the dimensionless ratio of these two pressures:

$$R_{max} = \frac{|P_{top}^{max}|}{|P_0|} \approx \frac{15 L_3^4}{e^2 \pi^2 L_1^2 L_2^2} = \frac{15}{4\pi^3 \alpha} \cdot \frac{L_3^4}{L_1^2 L_2^2}. \tag{41}$$

Even at this maximum, the ratio is tiny. Using the example values for the parameters that were mentioned earlier, we find $R_{max} \sim 10^{-7}$, a negligi-

ble contribution. It appears that any topological effect will be completely drowned out by the regular propagating degrees of freedom.

Before concluding this section, there are a number of remarks that can be made about these computations. The presence of the topological sectors produces a vacuum pressure with a positive sign, i.e. the plates will be repelled from each other. This is in contrast with the conventional Casimir effect, which manifests itself in this system as an attractive force. Also of note is the appearance of the coupling constant in the final expression. The inverse coupling constant in the exponent $\exp(-1/e^2)$ is a characteristic feature of quantum tunneling processes [12], which is consistent with our interpretation of the instantons as tunneling events between the degenerate vacua.

While eq. (41) may suggest that the topological Casimir effect can never be measured, it is still way too soon to give up hope. We have found that there is a real, physical force associated with the existence of topological sectors, even though it is small. On a compact manifold like a 4-torus, the gauge freedom of the electromagnetic theory causes a degeneracy of the vacuum state, that allows for a new type of tunneling excitations called instantons. The instantons are completely decoupled from the photons in the system and provide an extra contribution to the Casimir pressure, as given in eqs. (36, 38). This underlying topological vacuum structure is analogous to that of the non-Abelian Yang-Mills field of section 2.3, but is special in that it could be directly measured, at least in theory, through the topological Casimir effect.

Due to its unusual origin, the topological Casimir effect has some unique features that separate it from its conventional counterpart. It is these qualities that will hopefully make it possible to measure the effect in a lab, despite it being relatively tiny. Most significant is the sensitivity towards an external magnetic field, which interacts with the instantons and creates a type of theta vacuum. The conventional Casimir effect is not affected by an external field, making it a promising tool to probe the topological features of the theory. The next section will focus on the response of our system to such a magnetic field.

5 The External Magnetic Field as a Theta Parameter

Because the Topological Casimir effect is so much smaller than the conventional Casimir pressure, some sort of probe is needed to detect it: something that is sensitive to the topological sectors but not to the fluctuating photons. Fortunately such a thing exists, in the form of an external magnetic field. In this section I will show that the external field interacts with the instantons by shifting the energy levels of the excitations. Apart from affecting the topological pressure, this also induces a nonzero magnetic field in the system due to the presence of the topological sectors. Interestingly, the external magnetic field shows all the behavior of a topological theta term, as discussed in sections 2 and 3.

Classically, an external magnetic field should have no influence on the conventional Casimir effect, simply due to the linearity of the Maxwell equations. Electromagnetic modes do not interact with each other. On the level of QED it is possible to have photon-photon interactions, but they are greatly suppressed. The lowest order Feynman diagrams have four vertices. This suggests that any such interaction is proportional to the factor $\alpha^2 B_{ext}^2/m_e^4$, which is incredibly small. Even in an external field as large as 1 Tesla this amounts to an order of 10^{-20}, much smaller still than the topological contribution. The exact correction to the Casimir effect due to photon-photon interaction is calculated in [13], confirming this quick estimation.

Because of its negligible effect on the conventional Casimir pressure, the external magnetic field is an ideal tool to probe the topological properties of our system. In the rest of this section we will assume a constant field B_{ext} in the z-direction. First we will calculate how this modifies the partition sum, before looking at the various response functions of the system, such the induced magnetic field and the magnetic susceptibility.

5.1 Instantons in an External Field

Including a constant B_{ext} in our Euclidean action (29) is fairly straightforward[3]. The total magnetic field is now comprised of three parts: $\mathbf{B} = \mathbf{B}_q + \mathbf{B}_{top} + \mathbf{B}_{ext}$. The external field will add an uninteresting constant term B_{ext}^2 to the action, but more important are the cross terms. As mentioned

[3]Note that a magnetic field is invariant under a Wick rotation, unlike an electric field, so we do not have to worry about the physical interpretation of B_{ext} in the Euclidean action.

above the interaction term $\mathbf{B}_q \cdot \mathbf{B}_{ext}$ should vanish, which is clearly the case due to the periodicity of $\mathbf{B}_q$ over the domain of integration — just like in eq. (30). The conventional and topological parts are still decoupled, nothing has changed there. Explicitly we find

$$(B_z^{ext} + \frac{2\pi k}{L_1 L_2 e}) \cdot \int d^4x B_z^q = 0. \tag{42}$$

The conventional Casimir effect is unchanged and $\mathcal{Z}_0$ can be computed as normal. It is the last cross term that will be making the difference:

$$2\,\mathbf{B}_{top} \cdot \mathbf{B}_{ext} = \frac{4\pi k}{L_1 L_2 e}\, B_{ext}. \tag{43}$$

This new term is nonzero and depends on the topological sector k. It can be considered as a source term in the action, which will be useful later on. As a result, the energy levels of the instantons get shifted and the classical Euclidean action becomes

$$S_{top} \;=\; \beta L_1 L_2 L_3 \left(\frac{2\pi k}{L_1 L_2 e} + B_{ext} \right)^2 \;=\; \pi^2 \tau \left(k + \frac{\theta_{eff}}{2\pi} \right)^2, \tag{44}$$

where, in close analogy with eq. (17) from 2d electrodynamics, we have defined the effective theta parameter

$$\theta_{eff} = B_z^{ext} L_1 L_2 e. \tag{45}$$

The rest of the partition sum computations is the same as before. The prefactor $\sqrt{\pi\tau}$, that arises from the fluctuations around the instanton configuration and was derived via dimensional reduction, is unaffected by the external field. Inserting the shifted energy of eq. (44) into the partition sum (36) gives us the final expression

$$\mathcal{Z}_{top}(\tau, \theta_{eff}) \;=\; \sqrt{\pi\tau} \sum_{k \in \mathbb{Z}} \exp\left[-\pi^2 \tau \left(k + \frac{\theta_{eff}}{2\pi} \right)^2 \right] \tag{46}$$

Before studying the physical response functions of the system, a few remarks should be made about the interpretation of the effective theta parameter. At first sight it appears that θ_{eff} enters the partition sum in exactly the same way as in eq. (18), but there are some subtle differences. After all, eq. (18) was derived using the Hamiltonian approach in Minkowski space, whereas our analysis of the 4d system is all done in the Euclidean metric.

The description of instantons as tunneling configurations between topological sectors is not possible in Minkowski space and conversely, it is unclear how to solve the 4d system using canonical quantization like in section 3.1. This is problematic for our interpretation that the external magnetic field creates a theta vacuum. In the Euclidean path integral approach, a theta vacuum appears in the action as a complex weight of the topological sector, as seen in eqs. (7) and (26), rather than the shift of the energy levels that we find in (46).

To resolve this issue, consider the dual representation of (46) after Poisson resummation:

$$\mathcal{Z}_{top}(\tau, \theta_{eff}) \;=\; \sum_{n\in\mathbb{Z}} \exp\left[-\frac{n^2}{\tau} + i\,\theta_{eff}\,n\right]. \tag{47}$$

In this form, the role of the magnetic field as a theta parameter becomes more clear. The partition function is obviously 2π-periodic in θ_{eff}, which satisfies all the criteria of a topological theta term. As is necessary in Euclidean space, the theta term enters the expression as a complex phase and couples to the topological integer n. However, it should be emphasized that n does *not* label the original instantons that we constructed in section 4. Instead the terms in this series correspond to some kind of dual configurations, with a classical action proportional to τ^{-1}. This means that the θ-state created by the magnetic field cannot easily be described in terms of winding numbers and topological sectors.

From eq. (47) it follows that the asymptotic behavior is largely the same as in section 4.2. In the limit $\tau \to 0$, once again all topological features vanish as only the $n = 0$ term remains, leaving $\mathcal{Z}_{top} = 1$. The asymptotic limit $\tau \ll 1$ also includes the terms $n = \pm 1$ to yield:

$$\mathcal{Z}_{top} \;\approx\; 1 + 2\cos(\theta_{eff})\,e^{-1/\tau}\;, \qquad \tau \ll 1, \tag{48}$$

similar to (37). In the general case, we again need numerical tools to investigate the pressure and the magnetic behavior of the system.

5.2 Pressure and the Magnetic Response Functions

Now that the partition function is resolved, finding the topological pressure (38) is easy. To get a first impression of the external field's influence, let us look at the small-τ limit, where there is an analytical solution. Eq. (48) yields

$$P_{top} \approx \frac{e^2}{\beta^2 L_3^2}\,\cos(\theta_{eff})\,e^{-1/\tau}, \quad \tau \ll 1. \tag{49}$$

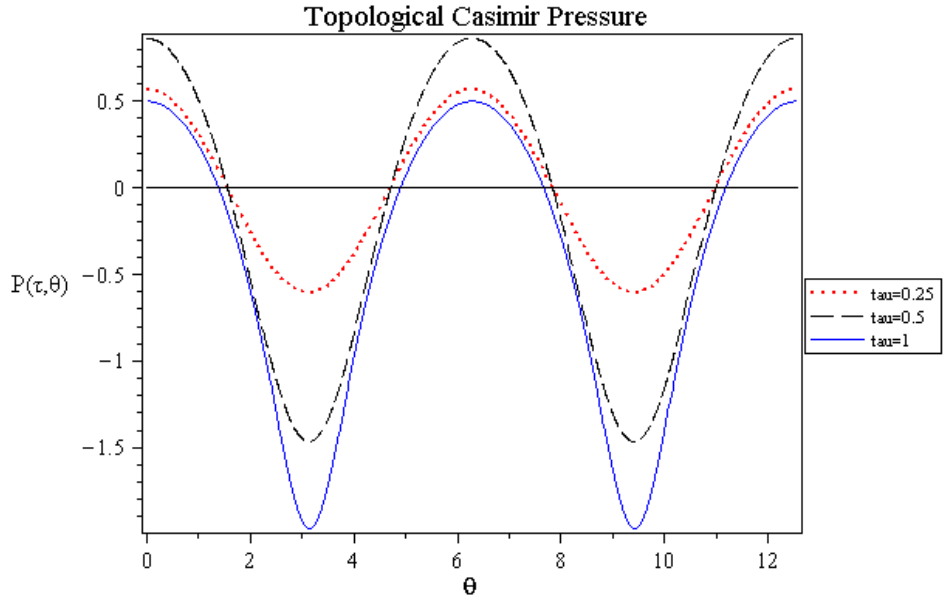

Figure 4: *A numerical plot of the topological Casimir pressure as a function of* $\theta_{eff} \equiv eL_1L_2B_{ext}$*, given in units of* $\frac{2}{L_1^2L_2^2e^2}$ *for three different values of* τ*. A clear* 2π *periodicity is seen and local extrema are between odd and even integer multiples of* π*.*

While the pressure is still exponentially suppressed, what is striking is the factor $\cos(\theta_{eff})$. This suggest that the force on the system will switch between being attractive and repulsive, depending on the strength of the external magnetic field $B_{ext} \sim \theta_{eff}$. The same thing is seen in Figure 4, a numerical plot of the topological pressure as a function of θ_{eff}, for various values of $\tau \simeq 1$.

Figure 4 also shows clearly the oscillatory behavior with respect to θ_{eff}. The extrema of the function are at integer multiples of π, with the odd multiples corresponding to a negative Casimir pressure. We see that, by playing around with the extra parameter θ_{eff}, it is possible to further amplify the topological Casimir effect. Unfortunately the increase is not enough to make a significant difference in comparison with the conventional pressure. A 3d plot shows a maximum pressure only few times larger than what we found in eq. (40).

However, the oscillating variation of the topological Casimir pressure

in an external magnetic field is a unique feature that might be possible to measure experimentally. It serves mainly to distinguish the topological contribution from the conventional Casimir effect, which is not sensitive to an external field. B_{ext} takes the role of a theta parameter by causing interference between the topological sectors. This shifts the energy spectrum of the instantons to produce the variation shown in Fig. 4.

In addition to changes in the topological pressure, it is interesting to study how B_{ext} affects the magnetic properties of the system. After all, the instanton excitations carry a magnetic field (28). In the case where $B_{ext} = 0$, the magnetic field configurations of instantons with opposite topological charge (but the same energy) will cancel each other, resulting in a vanishing net magnetic field. This can also be seen from symmetry arguments: without an external magnetic field the system is $\mathcal{P}$ and $\mathcal{CP}$ invariant, which means there can be no induced field. However, a nonzero theta parameter θ_{eff} is known to break these symmetries. The external magnetic field shifts the spectrum, such that instantons of opposite k have a different action and their corresponding magnetic fields no longer cancel in the partition sum. The result is an induced B-field that counteracts the applied magnetic field.

The expectation value of the total magnetic field of the system can be computed from the partition function as follows:

$$\langle B \rangle \;=\; -\frac{1}{\beta V}\cdot\frac{\partial}{\partial B_{ext}}\ln \mathcal{Z}_{top} \;=\; -\frac{e}{\beta L_3}\cdot\frac{\partial}{\partial \theta_{eff}}\ln \mathcal{Z}_{top} \tag{50}$$

The reasoning for this expression is similar to that for the pressure. If the free energy is lowered by changing the strength of the external magnetic field, then the system can emulate this by inducing its own magnetic field proportionally. This is also analogous to the calculation of expectation values in QFT, as the functional derivative of the partition function towards a source term[4]. If this argument does not convince you, we can insert the partition sum (46) into eq. (50) to explicitly find:

$$\langle B \rangle \;=\; \frac{\sqrt{\tau\pi}}{\mathcal{Z}_{top}}\sum_{k\in\mathbb{Z}}\left(B_{ext}+\frac{2\pi k}{L_1L_2e}\right)\exp\left[-\tau\pi^2(k+\frac{\theta_{eff}}{2\pi})^2\right], \tag{51}$$

which is intuitively clear as a thermodynamic expectation value. $B_{ext}+\frac{2\pi k}{L_1L_2e}$ is the total field strength of the configuration labeled by winding number k, while the exponential is its Boltzmann factor $e^{-\beta E}$. Dividing by $\mathcal{Z}_{top}$

[4]Except that in this case, the source is physical and is thus not set to zero after taking the derivative.

ensures the normalization and cancels the prefactor $\sqrt{\tau\pi}$. As mentioned above, when $B_{ext} = 0$ the series is antisymmetric in k and all terms will cancel in pairs.

In the limit $L_1 L_2 \to \infty$, all the topological effects vanish and we recover $\langle B \rangle = B_{ext}$ as expected. To see this, it is possible to rewrite eq. (51) as

$$\langle B \rangle \;=\; B_{ext} - \frac{e}{\beta L_3} \cdot \frac{\partial}{\partial \theta_{eff}} \ln \sum_{k \in \mathbb{Z}} \exp\left[-\tau\pi^2 k^2 - \tau\pi k \theta_{eff}\right]. \qquad (52)$$

The second term vanishes when $\tau \to 0$. Unfortunately this cannot be directly seen from the asymptotic expression (48), because of the way θ_{eff} depends on $L_1 L_2$.

Just as with the pressure, it is more enlightening to study a numerical plot of the induced field, for values of $\tau \simeq 1$. Such a plot is shown in figure 5. Again the oscillatory behavior is immediately obvious, which is consistent with the interpretation of the external magnetic field as a theta parameter.

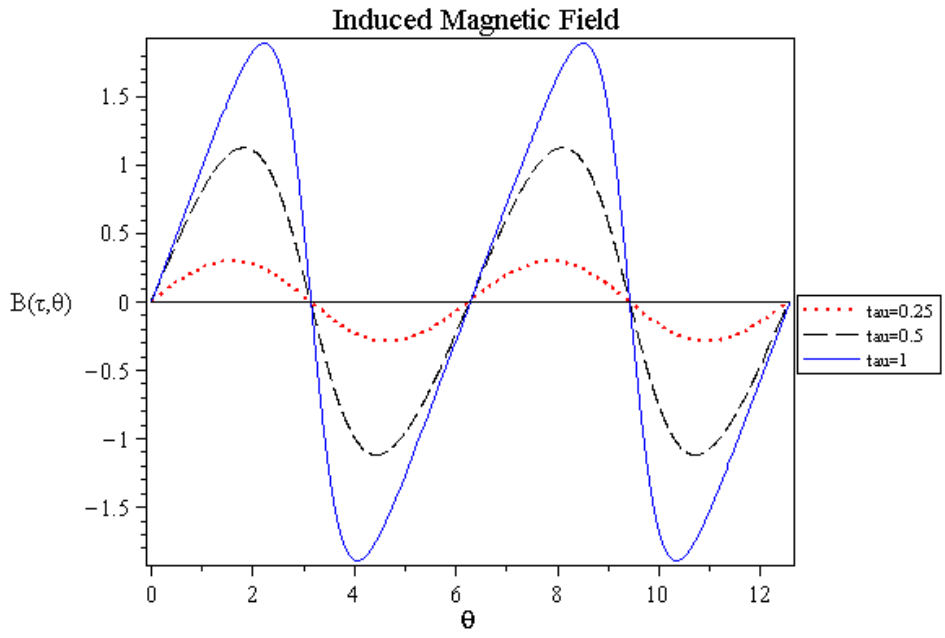

Figure 5: *A numerical plot of the induced magnetic field in units of* $\frac{1}{L_1 L_2 e}$ *as a function of* θ_{eff}*. The oscillatory behaviour becomes more pronounced for large* τ*.*

Furthermore, $\langle B \rangle$ vanishes when θ_{eff} reaches an integer multiple of π. This is particularly interesting because it means that, for a nonzero multiple of π, the external magnetic field is completely canceled by the contribution from the instantons.

The expression (50) for the expectation value of the magnetic field is very reminiscent of the way magnetization is computed in statistical physics. Up to a sign, $\langle B \rangle$ is equivalent to the magnetization per unit volume:

$$\langle m \rangle \;=\; \frac{1}{\beta V} \cdot \frac{\partial}{\partial H} \ln \mathcal{Z}, \tag{53}$$

where H is the magnetic field strength in the medium. This leads us to define the magnetic susceptibility of the system:

$$\chi_{mag} \;=\; -\frac{1}{\beta V} \cdot \frac{\partial^2}{\partial B_{ext}^2} \ln \mathcal{Z}_{top} \;=\; -\frac{2}{\tau} \cdot \frac{\partial^2}{\partial \theta_{eff}^2} \ln \mathcal{Z}_{top}. \tag{54}$$

The susceptibility represents the magnetic response of the free energy towards an external source, in this case the external magnetic field $B_{ext} \sim \theta_{eff}$. It is a dimensionless quantity (in natural units), as the right-hand side of eq. (54) shows. Because of this, we can easily use the asymptotic expression (48) to conclude that the susceptibility is again exponentially suppressed $\sim e^{-1/\tau}$ when $\tau \ll 1$. For the more general regime we must again resort to a numerical plot, seen in figure 6.

The plot of the magnetic susceptibility shows some very unique features. Most importantly, χ_{mag} flips sign such that the system will switch between being diamagnetic and paramagnetic, depending on the strength of the external field. This kind of behavior is not often seen in condensed matter systems. Furthermore, the susceptibility does not vanish when $\theta_{eff} = 0$. This makes sense intuitively, since χ_{mag} represents the sensitivity to an external magnetic field.

Not only are the induced magnetic field and the susceptibility of use for possible experiments, they also hold some theoretical interest. Because of the universality of topological theta terms, these quantities are very closely related to the ones of other topological systems. In the 2d electrodynamics from section 3, as well as 4d QCD mentioned in section 2.3, one can define a so-called *topological density* that is completely analogous to our induced magnetic field (50). Likewise, our magnetic susceptibility corresponds to the *topological susceptibility* of other systems with a theta term. The susceptibility plays a role even when $\theta = 0$, like in QCD where it is connected to the mass of certain mesons through the Witten-Veneziano relation. As such the

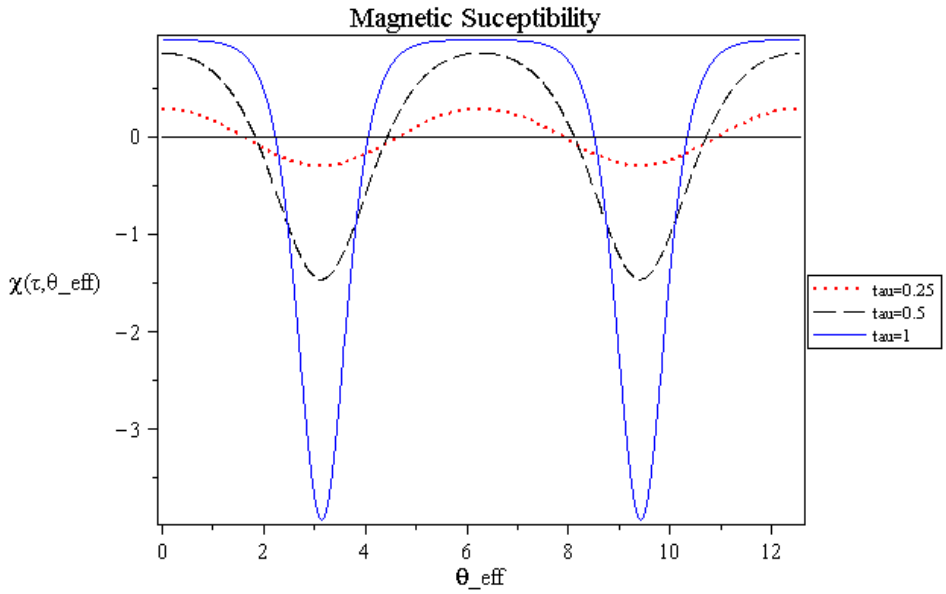

Figure 6: *A numerical plot of the magnetic susceptibility χ_{mag} as a function of θ_{eff} for different values of τ. It oscillates with θ_{eff} as it should and does not vanish at $\theta_{eff} = 0$. The magnetic susceptibility is dimensionless in natural units.*

topological Casimir effect allows us to indirectly investigate theories that are otherwise difficult to access.

To conclude this section, we have seen that an external magnetic field interacts with the topological Casimir effect. It takes the role of a topological theta parameter and the system shows all the universal behavior associated with this. The addition of the theta parameter modifies the topological pressure and the magnetic field of the system, both of which are periodic as a function of the external field strength. This very specific variation is something that could possibly be measured in a lab. The external magnetic field is an ideal tool to probe the topological features of our setup, since it leaves the conventional Casimir effect entirely unaffected. As such, the sensitivity towards an external field is a unique and integral part of the topological Casimir effect that sets it apart from other features of the quantum vacuum.

6 Discussion and Conclusion

The Casimir effect is an exciting new manifestation of topology in the quantum vacuum. It arises from tunneling configurations between the topological sectors, the degenerate vacuum states that are topologically different even though they correspond to the same physical state. However, all this theory means very little until the effect has been experimentally confirmed. In this work I have discussed several times the possibility of measuring the topological Casimir effect, but this should not be mistaken for an experiment proposal. A collaboration with an experimental physicist, somebody who knows what is and isn't possible in a lab, would be helpful for suggesting a realistic setup. Regardless, this thesis would not be complete without some short discussion on this matter.

Although I am generally optimistic that the topological Casimir effect can be observed, some major challenges would have to be overcome. The first question that readers are likely to ask themselves, is how one would create the Euclidean 4-torus that our theory is formulated on. It is important to keep in mind here that the system I discuss in the text is not intended to be the most general description of the topological Casimir effect. Instead, the 4-torus was chosen as the simplest configuration that demonstrates the essential features of the theory. For practical applications in the lab a slightly different setup may be useful. It is however probable that some sort of periodic boundary conditions are needed to realize the required nontrivial topology of the spacetime.

A Euclidean 4-torus corresponds to a 3-torus at finite temperature, as shown in appendix B.1. To create such a system, one must engineer a box with periodic boundary conditions on opposing sides, in all three directions. Please note though that the periodicity in the z-direction is not used in the derivation of section 4, so the same topological effects are possible without it. Creating periodicity in x and y-direction might be as simple as connecting these sides with a superconducting wire. Having the plates in the xz-plane and the yz-plane be metallic would still allow the magnetic field from the instantons in the z-direction. This setup would need a closer investigation before making any conclusions, though. Another option would be to create actual curved boundaries, like a ring or a 2-torus. Formulating the theory for such a configuration would be much more complicated. All things considered, I am convinced that with the current state of material science, it should be possible to create a system that exhibits the topological Casimir effect.

Of course, creating the system is only half the battle. Since the topo-

logical effects are so small, the actual detection will also be very difficult. Aside from the practical challenges of observing such a tiny effect, there are many corrections that need to be accounted for — even more so when dealing with real materials instead of idealized boundary conditions. The addition of an external magnetic field will add a distinctive variation to the Casimir pressure, but it will still be orders of magnitude smaller than the conventional Casimir effect. It would be interesting to see if one could generate physical photons from the induced magnetic field, for example by adding time-dependence to the external field, similar to the dynamical Casimir effect [14]. However, this subject needs further research to make any quantitative predictions. The experimental observation of the topological Casimir effect is still a long way off, but as of yet there is no reason to believe that it is impossible.

Assuming that the topological Casimir effect can be recreated in the lab, what would be the implications? Due to the universality of the topological behavior (see section 2), observation of the effect could tell us things about completely different systems. Topological Casimir experiments would provide a means to answer very fundamental questions about the quantum vacuum, not only in QED but also in QCD. An important example is the possible application in cosmology, where the topological Casimir effect has been suggested as a dark energy candidate [5, 16]. In this case the QCD vacuum, as described in section 2.3, yields a nonzero Casimir energy when defined on an expanding Hubble universe. An order of magnitude estimation of this energy is in very good agreement with the observed dark energy density. If true, this would be an amazing opportunity to test cosmological properties in a controlled environment, something that is quite rare.

In conclusion, there is interesting new physics that emerges when considering the electromagnetic field on nontrivial topological spaces. This effect is well established in $1 + 1$ dimensions: correspondence between the gauge group and the spacetime topology leads to the existence of topological sectors, labeled by an integer winding number. Instanton excitations provide tunneling between these sectors and their thermal fluctuations yield a nonzero vacuum energy. For a consistent theory it is necessary to sum over all winding numbers — all possible instantons — in the partition function.

In 2d QED, the topological excitations are the only degrees of freedom in the theory, since physical photons cannot exist. On the other hand, in four spacetime dimensions the topological vacuum energy must compete with the conventional Casimir energy, that originates from the zero-point energy of the photon modes. On the toroidal system that is discussed in this text, the topological Casimir effect is several orders of magnitude smaller than

its conventional counterpart. However, it may still be studied through some of its unusual properties, like the sensitivity towards an external magnetic field.

Under the influence of an external magnetic field, the topological Casimir effect shows a unique oscillating behavior as a function of the field strength. By varying the external field, one can switch between an attractive and repulsive Casimir force, or between a paramagnetic and diamagnetic system. The role of the external magnetic field here is directly analogous to the topological theta parameter in the QCD vacuum, or $\theta = \pi$ in strong topological insulators.

All in all, I think that this is a meaningful discovery that will have significant implications for our understanding of the quantum vacuum. The topological Casimir effect provides a direct means to experiment with the physics of topological sectors and theta states, opening the way to fascinating new research.

‘

References

[1] C. Cao, M. van Caspel and A.R. Zhitnitsky, Phys. Rev. D **87**, 105012 (2013).

[2] H.B.G. Casimir, Proc. Kon. Ned. Akad. Wetenschap **51**, 793 (1948).

[3] S.K. Lamoreaux, Phys. Rev. Lett. **78** 5 (1997);
U. Mohideen and A. Roy, Phys. Rev. Lett. **81**, 4549 (1998);
H.B. Chan et al., Science **291**, 1941 (2001);
G. Bressi et al., Phys. Rev. Lett. **88**, 041804 (2002);
S.K. Lamoreaux, Rept. Prog. Phys. **68**, 201 (2005);
G.L. Klimchitskaya et al., Rev. Mod. Phys. **81**, 1827 (2009).

[4] G. Plunien, B. Muller and W. Greiner, Phys. Rept. **134**, 87 (1986);
M. Bordag, U. Mohideen and V.M. Mostepanenko, Phys. Rep. **353** 1 (2001);
K.A. Milton, J. Phys. A **37** R209 (2004);
M. Bordag, G.L. Klimchitskaya, U. Mohideen and V.M. Mostepanenko, *Advances in the Casimir Effect*, Oxford University Press (2009).

[5] A.R. Zhitnitsky, Phys. Rev. D **86**, 045026 (2012)

[6] G. Kelnhofer, Nucl. Phys. B **867**, 110 (2013).

[7] B.S. DeWitt et al., Physica **96A**, 197 (1979);
C.J. Isham, Proc. Roy. Soc. Lond. A **362**, 383 (1978);
C.J. Isham, Proc. Roy. Soc. Lond. A **364**, 591 (1978);
R. Banach and J.S. Dowker, J. Phys. A **12**, 2527 (1979).

[8] M. Nakahara, *Geometry, Topology and Physics*, Institute of Physics Publishing (2003).

[9] M. Srednicki, *Quantum Field Theory*, Cambridge University Press (2007).

[10] I. Sachs and A. Wipf, Helv. Phys. Acta **65**, 652 (1992),
I. Sachs and A. Wipf, Annals Phys. **249**, 380 (1996),
S. Azakov, H. Joos and A. Wipf, Phys. Lett. B **479**, 245 (2000).

[11] S. Azakov, Int. J. Mod. Phys. A **21**, 6593 (2006) [hep-th/0511116].

[12] H. Suzuki and H. Yasuta, Phys. Lett. B **400**, 341 (1997).

[13] D. Robaschik et al., Ann. Phys. **174** 401 (1987).

[14] G. T. Moore, J. Math. Phys. **11**, 2679 (1970),
S. A. Fulling and P. C. W. Davies, Proc. R. Soc. London, Ser. A **348**, 393 (1976),
C. M. Wilson et al., Nature **479**, 376 (2011).

[15] D. F. Walls and G. J. Milburn, *Quantum Optics*, Springer (2008).

[16] A.R. Zhitnitsky, Phys. Rev. **D84**, 124008 (2011).

[17] M. Le Bellac, *Thermal Field Theory*, Cambridge University Press (2000).

Appendix A: The Conventional Casimir Effect

In this appendix I discuss some relevant points of the conventional Casimir effect, which is frequently compared to the topological contributions in the main text. None of the physics in this section is new, and in fact there have been many books written about the subject. The goal of this appendix is mainly to derive the Casimir pressure on a 4-torus, as given in eq. (31). Finite temperature corrections will also be discussed. For most other things, such as the Green's Function formalism or the subtle interpretation of regularization, the reader will be referred to several standard works [4].

A.1 2d Scalar Field

The Casimir effect arises from the quantization of a field within certain boundary conditions, which is different than in free Minkowski space. As an illustration, let us start with a simple massless scalar field $\phi(x,t)$ in 1+1 dimensions. Canonical quantization defines the field in terms of creation and annihilation operators, such that the operator $\hat{a}_k^\dagger$ creates a scalar particle of wave vector k. The number operator $\hat{n}_k = \hat{a}_k^\dagger \hat{a}_k$ counts the number of particles of wave vector k in the system. The Hamiltonian of the system is given by $H = \sum \hbar\omega_k(\hat{n}_k + 1/2)$, just as for a collection of quantum harmonic oscillators. We see that even in the vacuum where $n_k = 0$, each mode contributes a zero-point energy of $\hbar\omega_k/2$. In free Minkowski space, all wavelengths are allowed and k forms a continuous spectrum. The total vacuum energy on an interval of length L becomes:

$$E_{Mink}(L) = \frac{\hbar L}{2}\int_{-\infty}^{\infty}\frac{\mathrm{d}k}{2\pi}\omega_k. \tag{A.55}$$

Now we impose boundary conditions on the field, confining it to a box such that

$$\phi(0,t) = \phi(a,t) = 0. \tag{A.56}$$

As a result the allowed wavelengths are quantized, yielding $k_n = \pi n/a$ where n is a positive integer. The vacuum energy of the system within these boundaries now becomes:

$$E_{bound} \;=\; \frac{\hbar}{2}\sum_{n=1}^{\infty}\omega_{k_n} \;=\; \frac{\pi\hbar c}{2a}\sum_{n=1}^{\infty} n \tag{A.57}$$

This energy is divergent, but a finite quantity can be acquired by subtracting the Minkowski vacuum energy $E_{Mink}(a)$. This difference is known as the

Casimir energy $E_{cas} \equiv E_{bound} - E_{Mink}$. To compute the Casimir energy, we introduce a regulator $e^{-c\delta k}$ into the integral and sum, and then take the limit $\delta \to 0$ at the end. This gives us

$$E_{Mink} \;=\; \lim_{\delta\to 0}\; \frac{c\hbar a}{2\pi}\int_0^\infty \mathrm{d}k\, e^{-c\delta k} k \;=\; \lim_{\delta\to 0}\; \frac{\hbar a}{2\pi c\delta^2} \tag{A.58}$$

whereas the energy with boundaries yields

$$E_{bound} \;=\; \lim_{\delta\to 0}\; \frac{c\hbar\pi}{2a}\sum_{n=1}^{\infty} e^{-c\pi\delta n/a}\, n \;=\; \lim_{\delta\to 0}\; \frac{\hbar a}{2\pi c\delta^2} - \frac{\pi\hbar c}{24a}. \tag{A.59}$$

Subtracting E_{Mink} cancels the divergent term in the expansion and offers the Casimir energy

$$E_{cas} = -\frac{\pi\hbar c}{24a}. \tag{A.60}$$

Since the energy depends on the size of the box a, it produces a vacuum pressure. This is known as the Casimir effect. The method used here is called the *mode summation* technique and is intuitively the most clear. However, for more complicated systems this method might not work and one must resort to other tools, such as path integrals or the energy momentum tensor.

The result (A.60) can be obtained more easily using zeta function regularization. Using the analytical continuation of a zeta function, we can rewrite (A.57) as

$$E \;=\; \lim_{s\to 0}\; \frac{\pi\hbar c}{2a}\sum_{n=1}^{\infty} n^{s-1} \;=\; \lim_{s\to 0}\; \frac{\pi\hbar c}{2a}\zeta_R(s-1) \tag{A.61}$$

where the Riemann zeta function $\zeta_R(z)$ is defined as

$$\zeta(z) = \sum_{n=1}^{\infty} \frac{1}{n^z}. \tag{A.62}$$

Of course, in general the zeta function is only properly defined for $z \geq 2$, otherwise the series diverges. It is however possible to create an analytic continuation onto the complex plane, a technique that is very well studied. This continuation assigns a value of $\zeta_R(z)$ for any $z \in \mathbb{C}$. It suggests that $\zeta_R(-1) = -\frac{1}{12}$, which yields the same Casimir energy as in eq. (A.60). To prove this in a rigorous manner requires a lot of math and for that I will refer to the literature [4]. With some difficulty it can be shown that these

zeta function procedures are mathematically equivalent to the subtraction of the Minkowski vacuum energy and that it is more than just a useful trick. Other regularization schemes, like point-splitting, are also possible.

Aside from imposing fixed boundary conditions like eq. (A.56), one can also consider the Casimir effect on compact topological spaces. For example, when the scalar field $\phi(x,t)$ is defined on a ring of circumference a, the periodic boundary conditions cause quantization of the allowed momenta. The result is a Casimir energy similar to (A.60), up to a numerical factor. It is these periodic boundary conditions that cause the conventional Casimir effect on the 4-torus.

A.2 The EM Casimir Effect on a Torus

In section 4 the electromagnetic Casimir effect on a Euclidean 4-torus is discussed. The compactified time dimension, corresponding to a finite temperature, will not be considered for now. In the low temperature regime, the thermal correction is very small as we will derive at the end of this appendix. That leaves a 3-torus with size $L_1 \times L_2 \times L_3$, where $L_3 \ll L_1, L_2$.

Switching from a scalar field to the electromagnetic field does not change much, for the conventional Casimir effect with periodic boundary conditions. The two polarization directions act as independent massless scalar fields and only contribute a factor 2. This reduction to a scalar field is often possible, although for some boundary conditions the process is less trivial. Working from now on in natural units, the Casimir energy becomes:

$$E_{Cas} \;=\; \frac{1}{2}\sum_{\mathbf{k},\lambda} \omega_{\mathbf{k}}^{(\lambda)} \;=\; \sum_{\mathbf{k}} \omega_{\mathbf{k}}, \tag{A.63}$$

where λ denotes the polarization. Due to the periodic BCs, the momentum $\mathbf{k}$ is quantized. For the z-direction, this implies $k_z = 2\pi n/L_3$. Because L_1 and L_2 are much larger than L_3, we can use the approximation that k_x and k_y are continuous. This simplifies the computations a lot.

$$\omega_{n,k_{||}} = \sqrt{k_{||}^2 + \left(\frac{2\pi n}{L_3}\right)^2}\,, \qquad k_{||} \equiv \sqrt{k_x^2 + k_y^2} \tag{A.64}$$

To find the Casimir energy, we must integrate over k_x and k_y and sum over n. This expression can be transformed into another zeta function by using the parametric integral

$$\omega^{-s} = \int_0^\infty \frac{\mathrm{d}t}{t} \cdot \frac{t^{s/2}}{\Gamma(s/2)}\, e^{-t\omega^2}. \tag{A.65}$$

When inserted into the formula for the Casimir energy, this form allows us to integrate out $k_{||}$ and perform the zeta function regularization:

$$\begin{aligned}
E_{Cas} &= \lim_{s\to -1} \ \frac{L_1 L_2}{2\pi} \int_0^\infty \mathrm{d}k_{||}\, k_{||} \sum_n \omega_{n,k_{||}}^{-s} \\
&= \lim_{s\to -1} \ \frac{L_1 L_2}{2\pi} \ \sum_n \int_0^\infty \frac{\mathrm{d}t}{t} \cdot \frac{t^{s/2}}{\Gamma(s/2)} \int_0^\infty \mathrm{d}k_{||}\, k_{||} e^{-t(k_{||}^2 + \left(\frac{2\pi n}{L_3}\right)^2)} \\
&= \lim_{s\to -1} \ \frac{L_1 L_2}{2\pi} \ \sum_n \int_0^\infty \frac{\mathrm{d}t}{t} \cdot \frac{t^{s/2-1}}{\Gamma(s/2)} \, e^{-t\left(\frac{2\pi n}{L_3}\right)^2} \\
&= \lim_{s\to -1} \ \frac{L_1 L_2}{2\pi} \cdot \frac{\Gamma(s/2-1)}{\Gamma(s/2)} \ \sum_n \left(\frac{2\pi n}{L_3}\right)^{2-s} \\
&= \lim_{s\to -1} \ \frac{8\pi^2 L_1 L_2}{L_3^3} \cdot \frac{2}{2-s}\, \zeta_R(s-2) \ = \ -\frac{2\pi^2}{45} \cdot \frac{L_1 L_2}{L_3^3}.
\end{aligned} \tag{A.66}$$

With this bit of unpleasant algebra, we obtain the regularized vacuum energy of the torus. The final step is to compute the pressure in the z-direction, given by

$$P_{Cas} \ = \ -\frac{1}{L_1 L_2} \cdot \frac{\partial E_{Cas}}{dL_3} \ = \ -\frac{2\pi^2}{15 L_3^4}. \tag{A.67}$$

This is the expression used in section 4.2 to compare against the topological Casimir pressure. It is about an order of magnitude larger than the Casimir effect for parallel conducting plates (2), but the power law behavior is exactly the same.

In the above derivation we have neglected the periodic boundary conditions in the x and y-direction, by assuming that the momentum in those directions is continuous. Without that approximation, several corrections would be added to eq. (A.67) of the form $\sim \frac{1}{L_1^2 L_3^2}$ and $\sim \frac{1}{L_2^2 L_3^2}$. Compared to the leading order term, these are highly suppressed because L_1 and L_2 are much larger than L_3. We do not consider them further.

A.3 Thermal Corrections

Up until here, the Casimir effect computations of this appendix have been at zero temperature. Consider now the system at a finite temperature T. This causes thermal fluctuations which means that the modes of the electromagnetic field are no longer all in the ground state $n_k = 0$. In order to

define the free energy and pressure at finite temperature, it is necessary to compute the partition sum

$$\mathcal{Z} \;=\; \prod_{\mathbf{k},\lambda}\left(\sum_n \exp\left[-\beta\omega_{\mathbf{k}}(n+\frac{1}{2})\right]\right) \;=\; \prod_{\mathbf{k},\lambda}\frac{\exp[-\frac{1}{2}\beta\omega_{\mathbf{k}}]}{1-\exp[-\beta\omega_{\mathbf{k}}]}, \quad \text{(A.68)}$$

which yields the free energy

$$F = \sum_{\mathbf{k}}\left(\omega_{\mathbf{k}} + \frac{2}{\beta}\,\ln\left[1-\exp\left(-\beta\omega_{\mathbf{k}}\right)\right]\right). \quad \text{(A.69)}$$

The first term clearly corresponds to the Casimir energy (A.67) that has already been calculated, while the second term is known as the thermal correction. Interestingly, the correction term is convergent and does not need to be regularized. It is however still important to subtract the thermal vacuum energy of the space without the periodic conditions.

$$F_{Mink} \;=\; \frac{2V}{\beta}\int\frac{\mathrm{d}^3k}{(2\pi)^3}\ln\left[1-\exp\left(-\beta\omega_{\mathbf{k}}\right)\right] \;=\; -\frac{\pi^2 V}{45\,\beta^4} \quad \text{(A.70)}$$

This is simply the free energy of black-body radiation as given by basic statistical mechanics.

Computing the thermal correction for the torus is not trivial, but can be done in the low-temperature limit.

$$F^{therm} = \frac{L_1L_2}{\pi\beta}\int_0^\infty \mathrm{d}k_{||}\,k_{||}\sum_n \ln\left[1-\exp\Big(-\beta\sqrt{k_{||}^2+\left(\frac{2\pi n}{L_3}\right)^2}\Big)\right] \quad \text{(A.71)}$$

Assuming $\beta \gg L_3$, we can use the approximation $\ln\left[1-e^{-\beta\omega}\right] \approx -e^{-\beta\omega}$ as long as $n \neq 0$. Keeping only the terms with $n = 0, \pm 1$ the integral can be performed to find

$$F^{therm} \approx \frac{L_1L_2}{\pi\beta}\left[\frac{\zeta_R(3)}{\beta^2} - \frac{4\pi}{\beta L_3}\,\exp\left(-\frac{2\pi\beta}{L_3}\right)\right] \quad \text{(A.72)}$$

Subtracting the background energy F_{Mink} and calculating the corresponding pressure finally yields the small thermal correction for low temperatures:

$$P_{Cas}^{therm} \approx -\frac{\pi^2}{45\beta^4} + \frac{8\pi}{\beta L_3^3}\,\exp\left(-\frac{2\pi\beta}{L_3}\right) \quad \text{(A.73)}$$

Appendix B: Mathematical Tools

B.1 Wick Rotation and Thermal Field Theory

The Wick rotation is a crucial part of the path integral approach for describing quantum field theory at finite temperature. It transforms a problem in 3+1 dimensional Minkowski space into one formulated in 4d Euclidean space, by switching to an imaginary time coordinate [17]. The technique is motivated by the similarities between the partition function as defined in QFT, and the statistical partition function:

$$\mathcal{Z}_{QFT} = \int \mathcal{D}\phi \; e^{i\int \mathrm{d}t\, L[\phi]} \quad \longleftrightarrow \quad \mathcal{Z}_{stat} = \int \mathcal{D}m \; e^{-\beta H[m]} \tag{B.74}$$

where ϕ is a quantum field and m some kind of local order parameter.

Consider a field in 4d Minkowski space. The metric of the coordinates is $x_\mu x^\mu = t^2 - |\mathbf{x}|^2$. Now we apply the transformation

$$t \quad \longrightarrow \quad \tau \equiv -it \tag{B.75}$$

which produces the Euclidean 4-vector product: $|x_E|^2 = \tau^2 + |\mathbf{x}|^2$. In other words, the transformation switches between a Minkowski and a Euclidean metric. How would such a transformation affect the action of the system? For example, for a free scalar field we find:

$$\int \mathrm{d}^4x \left(\frac{1}{2}\left(\partial_\mu\phi\right)^2 - \frac{1}{2}m^2\phi\right) \quad \longrightarrow \quad i\int \mathrm{d}\tau\, \mathrm{d}^3x \left(\frac{1}{2}\left(\partial_\mu\phi\right)_E^2 + \frac{1}{2}m^2\phi\right) \tag{B.76}$$

The transformed integrand is known as the Euclidean Lagrangian L_E. The factor i cancels with the one in the partition sum. Note that the terms of L_E are typically real, since the Lagrangian only contains even powers of ∂_t. The exception are topological theta terms, as seen in eq. (7). The Wick rotated partition sum becomes

$$\mathcal{Z}_{QFT} = \int \mathcal{D}\phi \; e^{-\int \mathrm{d}\tau\, L_E[\phi]}. \tag{B.77}$$

To introduce the finite temperature into this expression, there is only step left: we identify the imaginary time with the inverse temperature β.

$$\mathcal{Z}(\beta) = \int \mathcal{D}\phi \; e^{-\int_0^\beta \mathrm{d}\tau\, L_E[\phi]}. \tag{B.78}$$

Here it is necessary that the fields ϕ that one integrates over satisfy the periodic boundary conditions $\phi(\tau = 0) = \phi(\tau = \beta)$. That why we considered a Euclidean 2-torus and 4-torus in sections 3 and 4 respectively, the

imaginary time component is also periodic in nature. For a more rigorous derivation, one can analyze the partition sum $\mathcal{Z} = \mathrm{Tr}[\exp(-\beta H)]$ to arrive at eq. (B.78).

B.2 Poisson Resummation

The Poisson Sum formula, in the form that was used many times in this work, is a result from Fourier analysis that states

$$\sum_{n=-\infty}^{\infty} \exp\left[-a\,(n+x)^2\right] \;=\; \sqrt{\frac{\pi}{a}} \sum_{k=-\infty}^{\infty} \exp\left[-\frac{\pi^2 k^2}{a} + 2\pi\, i\, x\, k\right]. \quad \text{(B.79)}$$

for positive a. Here we will show a quick proof.

Consider the sum $\sum_n f(n+x)$, for some function $f(x)$. This sum is periodic in x, with period 1. As a result it can be written in terms of discrete Fourier coefficients:

$$\sum_{n=-\infty}^{\infty} f(n+x) = \sum_{k=-\infty}^{\infty} c_k\; e^{2\pi\, i\, k\, x} \quad \text{(B.80)}$$

where the coefficients c_k are defined as

$$\begin{aligned} c_k \;&\equiv\; \int_0^1 \mathrm{d}x \sum_{n=-\infty}^{\infty} f(n+x)\; e^{-2\pi\, i\, k\, x} \\ &=\; \sum_{n=-\infty}^{\infty} \int_n^{n+1} \mathrm{d}x\; f(x)\; e^{-2\pi\, i\, k\, x} \\ &=\; \int_{-\infty}^{\infty} \mathrm{d}x\; f(x)\; e^{-2\pi\, i\, k\, x} \\ &=\; \hat{f}(k) \end{aligned} \quad \text{(B.81)}$$

with $\hat{f}(k)$ the Fourier transform of $f(x)$. Substituting this into eq. (B.80) yields

$$\sum_{n=-\infty}^{\infty} f(n+x) = \sum_{k=-\infty}^{\infty} \hat{f}(k)\; e^{2\pi\, i\, k\, x}. \quad \text{(B.82)}$$

Now we can choose for $f(x)$ the Gaussian

$$f(x) = e^{-ax^2} \quad \longrightarrow \quad \hat{f}(k) = \sqrt{\frac{\pi}{a}}\, e^{-\frac{\pi^2 k^2}{a}}. \quad \text{(B.83)}$$

Inserting this into eq. (B.82) recovers precisely the formula (B.79) that we wanted to prove.